COMPDYN 2013
4th ECCOMAS Thematic Conference on
Computational Methods in Structural Dynamics and Earthquake Engineering
M. Papadrakakis, N.D. Lagaros, V. Plevris (eds.)
Kos Island, Greece, 12–14 June 2013

FINITE ELEMENT MODEL UPDATING OF A FOOTBRIDGE BASED ON STATIC AND DYNAMIC MEASUREMENTS

Mario Solís[1], Leqia He[2], Geert Lombaert[2] and Guido De Roeck[2]

[1] E.T.S. Ingeniería - Universidad de Sevilla
Camino de los Descubrimientos s/n, 41092 Sevilla (Spain)
e-mail: msolis@us.es

[2] Structural Mechanics Division, KU Leuven
Kasteelpark Arenberg 40, bus 2448, B 3001 Heverlee, Belgium
e-mail: {Leqia.He, Geert.Lombaert, Guido.Deroeck}@bwk.kuleuven.be

Keywords: Footbridge, Model updating, Static response, Operational Modal Analysis, Foundation contribution

Abstract. *The Palmas Altas footbridge is a recently built bridge in Sevilla (Spain) designed by architect Richard Rogers. It is a 78.6m long steel-concrete box girder. The bridge has three spans, with two pairs of intermediate oblique piers. The cross section of the box girder and the piers are variable along the bridge length. The footbridge has a cylindrical roof with a complex structural geometry, made of elliptical crossing bars and a cylindrical shell. Before being taken in use, the structural response of the footbridge was experimentally identified by an operational modal analysis. Mode shapes and frequencies have been clearly identified. In addition, the static response of the structure was obtained from a static load test. A detailed finite element model has been built for analyzing both the static as well as dynamic behavior of the bridge. A model updating process has been performed to improve static and dynamic response predictions. The present analysis is mainly focused on the in plane behavior of the bridge, for which both static and dynamic experimental information is available. Special attention is paid to the role of the bearings and foundations in the structural response. It is shown that the measured static response provides useful information about the response of the bridge and its foundation, which is not available from a dynamic analysis only.*

1 INTRODUCTION

In the last decade, new civil engineering design challenges have emerged from the construction of new footbridges [1, 2]. Due to the small service loads, they are usually light and slender structures that must withstand dynamic loads from pedestrians, wind, and traffic or water flow underneath. Some structural dynamics problems are arising, including human induced vibrations and human-structure interaction. These problems have to be addressed and new design guidelines are required. For this purpose, information about the behavior of footbridges has to be collected and analyzed.

Experimental information about the behavior of a civil engineering structure can be obtained from Operational Modal Analysis (OMA). The experimental modal parameters give information about the actual properties of the structure and can be compared to predicted values from numerical models. By performing a model updating, a more accurate and realistic model can be obtained. The updating process can be used to understand the actual behavior of the structure.

This paper presents the updating process of a recently constructed footbridge in Sevilla (Spain). A detailed finite element model of the structure has been built to obtain a good approximation of the real structural response. The experimental identification includes an OMA and a static load test. The paper includes not only the dynamic response but also the static one in the updating process. Special attention is paid to the influence of the neoprene bearings, foundations and structural contribution of architectural elements. Useful information is obtained about the foundation contribution when combining the satic and dynamic response in the model updating.

The paper is organized as follows. The next section describes the structure and the finite element model. In the third section, the experimental results from the static and dynamic tests are presented. The model updating process and the discussion of the most significant results are presented next. Finally, some remarks and conclusions are drawn from the results.

2 Description of structure and FE model

The footbridge is a three-span steel box girder bridge built in Sevilla (Spain) in 2011. The bridge is 78.65 m long, including the main span of 39.15 m and two equal side spans of 19.25 m. Fig. 1 shows a side and perspective view of the bridge. The bridge is simply supported at both abutments and is also supported by two pairs of intermediate oblique piers. A detailed finite element model of the bridge was built to represent its structural response.

Figure 1: The Palmas Altas footbridge.

Fig. 2 shows the standard cross section of the bridge and a front view of one of the bridge ends. The cross section contains a steel box girder with a concrete slab of 150 mm thickness. The geometry of the girder is changing along the bridge, providing more stiffness towards the joints with the piers. The height of the girder varies from 0.56 m to 1.32 m, the thickness of the upper flange (steel part of the deck) varies from 12 to 20mm, the thickness of the bottom flange varies from 10 to 20mm and the thickness of the webs varies from 10 to 20 mm. Fig. 2(c) shows a schematic drawing of a side view of the bridge, including the foundation of the abutments and the piers. The foundations consist of a pile cap and 4 piles of 850 mm diameter and a length of 20 m (the drawing does not include the whole piles). A concrete beam connects the foundation of piers and abutments at both sides.

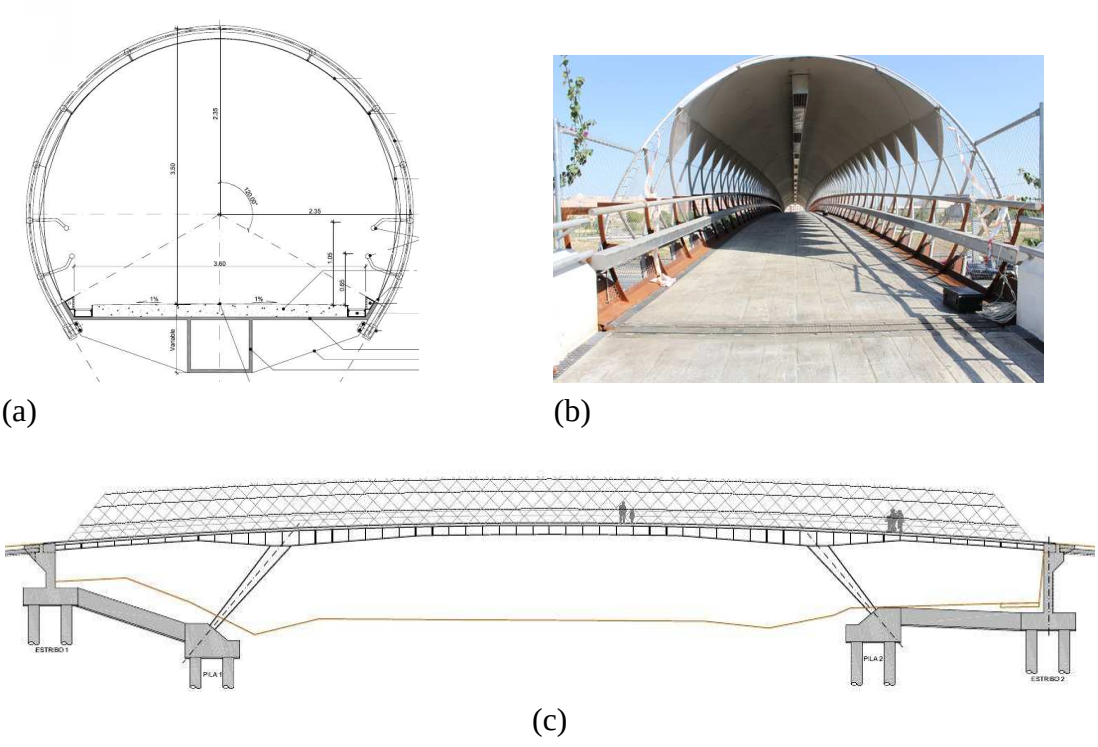

Figure 2: (a) Standard section of the bridge (b) Front view of one end of the bridge (c) Lateral drawing of the bridge including foundation

The triangular stiffeners of the girder (16 mm thickness) are located every 1.30m along the bridge. Inside the concrete slab, there are 5 longitudinal bar stiffeners and also one transversal bar stiffener every 1.30m. There is also one longitudinal stiffener on the bottom flange of the box girder and transversal stiffeners inside the box girder every 1.30m.

The roof consists of a cylindrical cover along the bridge. It is formed by elliptical inclined arched bars, geometrically defined as inclined sections of the cylindrical cover along the bridge. There are arched bars with two different orientations, so that the final assembly looks like a kind of three dimensional arched truss.

The roof provides a singular aesthetic appearance to the bridge and is an element of a clear major architectural significance. However, its structural contribution was not that clear. It was originally not considered as part of the structure in the design phase of the footbridge. However, its final construction design (robust bars and anchorage to the deck) makes the roof a significant

structural element, as found from the numerical and experimental analysis.

The piers are inclined, tapered and with a hollow cross section. The cross section of the piers varies from 0.5 mx0.5 m at the bottom to 0.4 mx1.62 m on top. The wall thickness is 20 mm. It must be noted that the South pier (5.125 m height) is shorter than the North pier (6.35 m height). Because of that, there is a lack of symmetry in the bridge.There are also 4 longitudinal and 3 transversal bar stiffeners inside the piers.

Fig. 3 shows a three dimensional representation of the finite element model. The whole girder as well as the piers are modeled with shell elements. Their internal bar stiffeners are modeled with beam elements. The concrete slab and the steel counterpart of the girder are modeled as a shell with composite material properties. The composite material is defined by one layer of concrete and one layer of steel. For the roof, curved 3 node bar elements and curved 8 node shell elements were used to represent its complex curved geometry.

The mechanical properties for steel and concrete in the finite element model are, respectively: Young's modulus $E = 210$ GPa and $E = 31.1$ GPa, density $\rho = 7850\ \mathrm{kg/m^3}$ and $\rho = 2400\ \mathrm{kg/m^3}$, Poisson modulus $\nu = 0.3$ and $\nu = 0.15$.

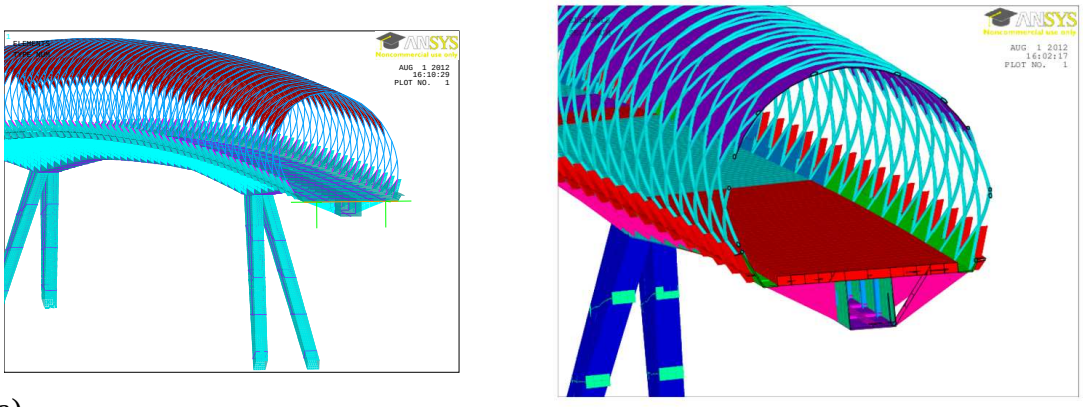

(a) (b)

Figure 3: (a) General view of the finite element model (b) Three dimensional representation of cross section

3 Experimental Analysis

3.1 Static load test

After construction, the bridge was subjected to a static load test. An equivalent load of $250\ \mathrm{kg/m^2}$ was applied by putting cement bags on top of the bridge deck (Fig. 4a). Vertical displacements were measured at eleven points along the bridge with a total station laser theodolite (Fig. 4b). Fig. 4c shows the measured displacements. It can be observed that there were significant vertical displacements on top of the piers. This behavior can only be explained by some displacements occurring at the foundations of the piers. This phenomenon and its implications on the updating process will be further discussed in the following sections.

3.2 Operational Modal Analysis

The dynamic properties (natural frequencies and mode shapes) of the bridge were obtained from an Operation Modal Analysis. The experimental test was carried out before the structure

(a)

(b)

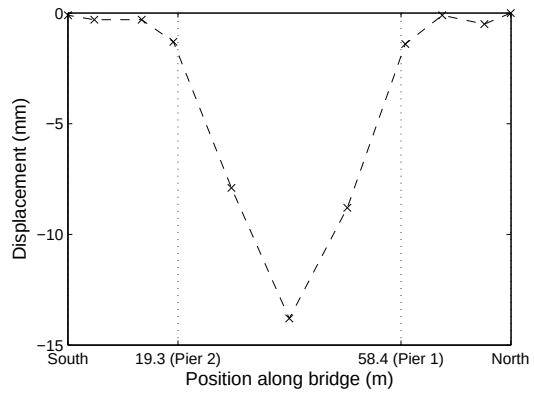

(c)

Figure 4: (a) Applied load (b) Static measuring equipment (c) Experimental displacements

was taken in use. It was only subjected to ambient vibration produced mainly by road traffic of the highway underneath the bridge.

In total, the dynamic response at 27 points was measured (Fig. 5c). The measurement nodes were located on top of the bridge deck (Fig. 5b). Accelerations in three directions were collected by triaxial wireless units (Fig. 5a). Three of the measurement points (11, 12 and 16 in fig.5c) were reference nodes that were measured by sensors with fixed locations. The other nodes were measured by nine roving sensors through 3 setups. One longitudinal line of measuring points, in addition to the reference nodes, was considered for each setup. The measurement duration was 15 minutes in each setup.

The measured vibration data were analyzed using MATLAB toolbox MACEC [3]. System identification was performed for each setup using the reference based covariance driven stochastic subspace identification algorithm (SSI-cov) [4].

In the following, modes below 10Hz are considered, as these are of most interest for ambient excitation and human induced vibrations. Table 1 shows the identified frequencies and damping ratios of the mode shapes in that frequency range. The table also includes information about the standard deviation of frequencies and damping ratios, and the Modal Phase Collinearity [5]. These parameters provide information about the stability and quality of the modal results.

The mode shapes are presented in fig. 6. Besides giving a three dimensional view of the deck, the vertical and horizontal movements of the three longitudinal lines of measuring points are shown as well. Torsional, vertical bending or lateral bending components of each mode can be observed.

It can be seen that the first mode is at 2.364 Hz and combines lateral and torsional movements of the bridge. The lateral bending component of this first mode is very similar to that of the third mode (3.298 Hz) but the latter does not show any torsional behavior. Additional measuring points on the roof would give complementary information about these modes and allow a clearer distinction between these modes. From the FE model results, it could be observed that the first mode is mainly a lateral mode of the roof, which leads to a lateral and torsional deformation of

(a)

(b)

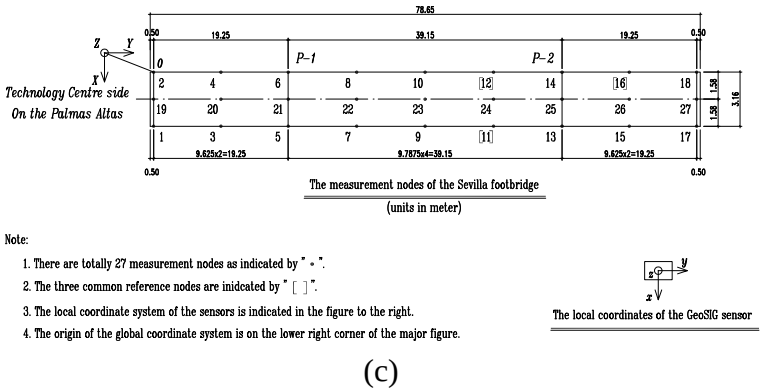

(c)

Figure 5: (a) Set of wireless sensor units (b) Sensor units during measuring process (c) Scheme of measuring points distribution

Mode Number	Freq (Hz)	Std. Dev. Freq.(%)	Damping ratio (%)	Std. Dev. damp.	M.Ph. Coll.	Description
1	2.364	0.001	0.23	0.01	1.00	Torsion + lat. bending
2	3.038	0.005	0.58	0.03	1.00	1^{st} bending.
3	3.298	0.006	1.11	0.19	0.99	First lateral bending
4	3.656	0.020	1.60	0.02	0.99	2^{nd} bending.
5	5.461	0.019	1.05	0.22	0.96	Lateral bend + torsion
6	5.727	0.008	0.92	0.07	0.97	Symmetric to 5
7	6.574	0.018	1.18	0.35	0.98	4^{th} bending.
8	6.903	0.031	1.75	0.14	0.95	Lat. bending
9	7.326	0.010	1.36	0.48	0.95	5^{th} bending
10	8.622	0.007	0.42	0.07	0.94	Torsion + lat. bend
11	8.855	0.018	1.05	0.07	0.98	6^{th} bending

Table 1: Identified modes from Operational Modal Analysis below 10Hz

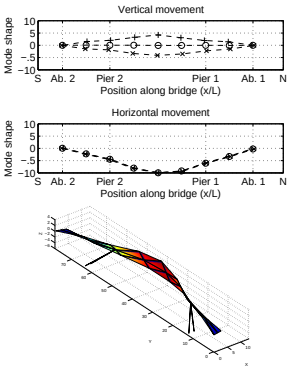

Mode 1 (2.364Hz)

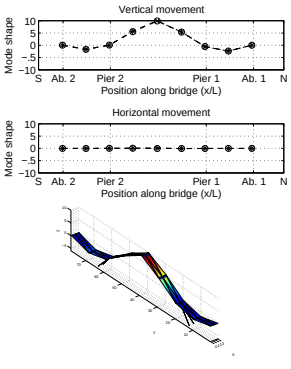

Mode 2 (3.038Hz)

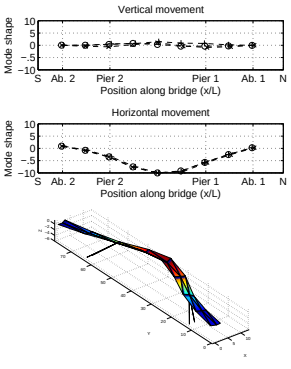

Mode 3 (3.298Hz)

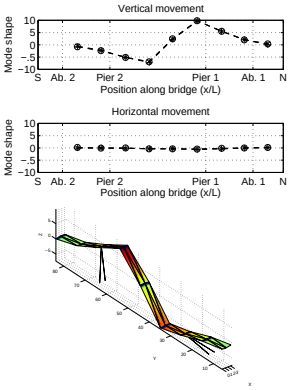

Mode 4 (3.656Hz)

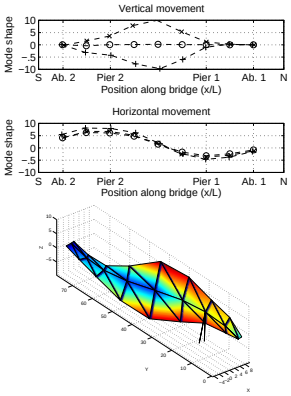

Mode 5 (5.461Hz)

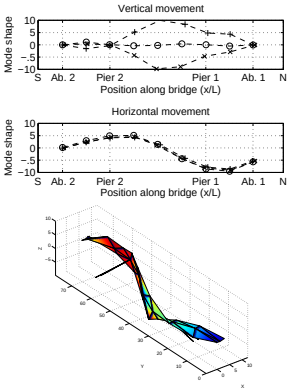

Mode 6 (5.727Hz)

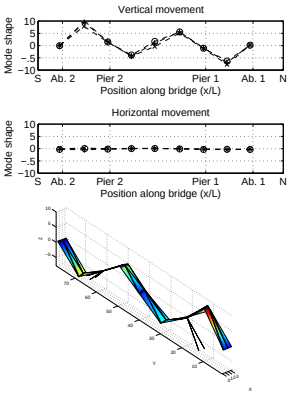

Mode 7 (6.574Hz)

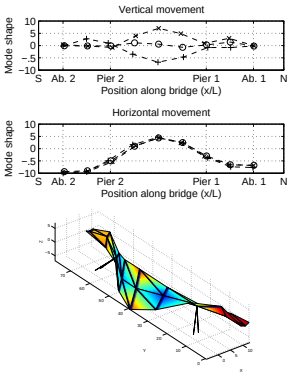

Mode 8 (6.903Hz)

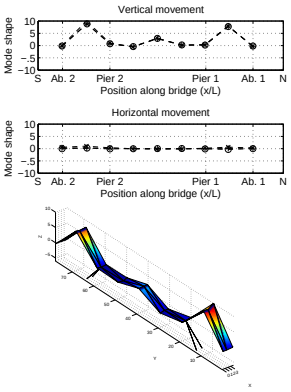

Mode 9 (7.326Hz)

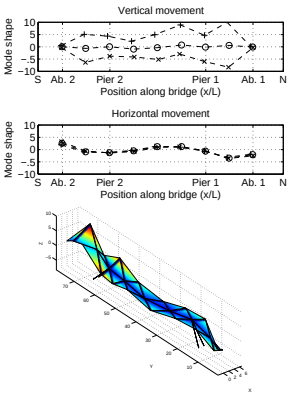

Mode 10 (8.622Hz)

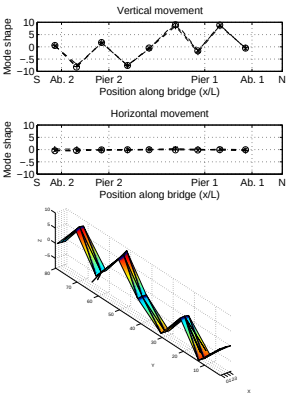

Mode 11 (8.855Hz)

Figure 6: Identified mode shapes from OMA

the deck. The third mode is a lateral mode of the whole bridge. If the roof is not considered in the FE model, only one of these modes is obtained (mainly a lateral bending mode). So it seems that the roof must be considered as part of the structure in order to obtain results in good agreement with the experimental observations. If it is considered as a non-structural element the number of mode shapes would be underestimated and the model would not be realistic [6].

Similar lateral and torsional deformation is also present in modes 5 (5.461 Hz) and 6 (5.727 Hz). They are second type lateral bending modes, with high lateral modal displacements at only one of the abutments. Mode 8 ($6.903Hz$) is a higher order lateral bending mode, including high modal displacements at both abutments. For all these lateral bending modes, the movement of the roof produces also a torsional deformation of the deck. Finally, there a pure torsional mode is found at 8.622 Hz (mode 10).

Regarding the vertical bending modes, the first one is mode 2 (3.038 Hz) and the second ones is mode 4 (3.656 Hz). It is worth to mention that the second bending mode, which is an antisymmetric mode, shows very high longitudinal modal displacements, including a high movement on top of the piles. Maximum longitudinal displacements values are 60% of the maximum vertical displacement. This illustrates how important it can be to take longitudinal movements into account when performing a modal analysis. This component of displacements is often neglected and can provide significant information about the behavior of the bridge, which should be considered for model updating.

Modes 7 (6.574 Hz) and 11 (8.855 Hz) are bending modes of higher order. There is also another bending mode which consists of a bending of both side spans (mode 9 at 7.326 Hz).

To resume, out of the 11 mode shapes identified below 10 Hz, 5 are vertical bending modes, 4 are lateral bending combined with torsional modes, and only 2 are purely torsional and purely lateral bending, respectively. In this paper, the 5 vertical bending modes will be the most relevant for combination with the in plane static bending response during the model updating.

The modal transfer norm [5] obtained for each mode gives information about their relevance in the measured response. According to that parameter, the most important modes in the ambient vibration response are (in order of relevance) the first bending mode (mode 2), the first lateral and torsion mode (mode 1) and the second bending mode (mode 4).

Fig. 6 also includes the MAC matrix for the eleven presented modes. The MAC matrix is almost diagonal, showing that the identified modes are mostly orthogonal. However, a high MAC value is observed between modes 1 and 3. As previously explained, these modes contain a significant roof motion. Because of the lack of measuring points on the roof, it is hard to distinguish between both modes.

4 MODEL UPDATING PROCESS

4.1 Objective function

The model updating process is used to solve an inverse problem so that the finite element model reproduce the experimental static and dynamic response of the structure as close as possible to the real (experimental) one. An optimization problem must be solved for which an objective function and updating parameters have to be properly chosen [7]. The objective function includes the difference between the experimental and numerical results. In this applications the objective function can be written as follows

$$\mathbf{p}^* = \arg\min_{\mathbf{p}} \frac{1}{2} \left[\sum_i \left[w_s r_i^s(\mathbf{p}) \right]^2 + \sum_j \left[w_f r_j^f(\mathbf{p}) \right]^2 + \sum_j \left[w_M r_j^M(\mathbf{p}) \right]^2 \right] \tag{1}$$

where $\mathbf{p}$ is the set of updating parameters, r_i^s is the residuals of the static displacement at measuring point i, r_j^f is the residual of frequency of mode j, and r_j^M is the residual of the MAC value of mode j. w_s, w_f and w_M are the weights applied to the residuals of static displacements, frequencies and mode shapes (MAC), respectively. The values of the weights are chosen in order to have good convergence and a trade-off between the influence of each part on the value of objective function, so none of them becomes dominant in the optimization process.

The residuals of the static displacement at each measuring point are defined as

$$r_i^s(\mathbf{p}) = \frac{u_i^s(\mathbf{p}) - \tilde{u}_i^s}{\tilde{u}_{max}^s} \tag{2}$$

where $u_i^s(\mathbf{p})$ is the displacement computed from the finite element model, $\tilde{u}_i^s$ is the experimental result and $\tilde{u}_{max}^s$ is the maximum experimental displacement.

The frequency residuals can be written as

$$r_j^f(\mathbf{p}) = \frac{f_j(\mathbf{p}) - \tilde{f}_j}{\tilde{f}_j} \tag{3}$$

where $f_j(\mathbf{p})$ is the computed natural frequency and $\tilde{f}_j$ is the corresponding experimental one of mode j.

The residuals in mode shapes computed is computed through the MAC values as follows:

$$r_j^M(\mathbf{p}) = 1 - MAC(\phi_j(\mathbf{p}), \tilde{\phi}_j) \tag{4}$$

where $\phi_j(\mathbf{p})$ is the computed mode vector j and $\tilde{\phi}_j$ is the corresponding experimental one.

The optimization problem is solved using a Newton trust region method, which is a gradient based iterative algorithm. The jacobian of the objective function is computed numerically using a finite difference scheme. One of the key issues in a model updating based on modal results is the matching of the computed and the experimental modes. In this paper, each experimental mode is paired to the computed mode that gives the highest MAC value.

4.2 Updating parameters

A detailed finite element model of the structure is set up to give a good approach of the behavior of the structure. However, the response is highly influenced by the actual boundary conditions, which could deviate form the idealized case. Therefore, the updating process considers equivalent springs simulating the contribution of the foundation. The stiffness values of these springs are considered as updating parameters. This paper focuses on the in plane static and dynamic behavior of the bridge, so that a total of 6 stiffness constants considered in the analysis. Fig. 7 show an schematic representation of the updating parameters. In the definition of the updating parameters, it has been assumed that the abutments and pier foundations at both sides of the bridge have the same stiffness.

The footbridge is supported by neoprene bearings at both ends. Based on the dimensions of the rubber and the steel layers [8, 9], the stiffness of each neoprene bearing in the vertical direction (k_{N-V}), transversal direction (k_{N-L}) and rotation ($k_{N-\theta}$) is estimated to be in the range $[1e8 - 1e9]$ N/m, $[1e6 - 2e6]$N/m and $[5e5 - 1.5e6]$N/m respectively.

Regarding the foundation of piers (4 piles of $850mm$ diameter and 20m long), an estimation of the equivalent horizontal (k_{P-L}), vertical (k_{P-V}) and rotational ($k_{P-\theta}$) stiffness of the piles working together as cantilever beams is 9.2×10^6N/m , 16×10^{10} N/m and 35×10^{10} Nm/rad

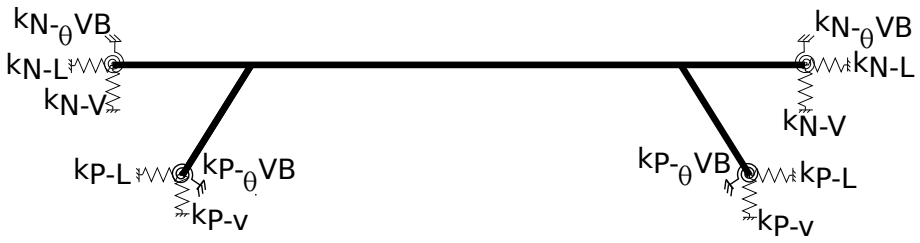

Figure 7: Schematic representation of the springs at foundations of the piers and abutments considered as updating parameters

	Case							
Parameter (N,m)	1	2	3	4	5	6	7	8
k_{N-V}	∞	5e8	5e8	5e8	5e8	5e8	5e8	5e8
k_{N-L}	0	1.5e6	1.5e6	1.5e6	1.5e6	1.5e6	1.5e6	1.5e6
$k_{N-\theta VB}$	0	1e6	1e6	1e6	1e6	1e6	1e6	1e6
k_{P-V}	∞	∞	1e9	1e8	∞	∞	∞	∞
k_{P-L}	∞	∞	∞	∞	∞	∞	1e8	1.5e7
$k_{P-\theta VB}$	∞	∞	∞	∞	∞	1e8	∞	∞

Table 2: Different combinations of values of updating parameters for manual calibration based on the static response

respectively. These values are considered only as estimated references and realistic values for the equivalent springs. The actual values of equivalent stiffness should be higher due to the soil contribution.

5 STATIC RESPONSE ANALYSIS

5.1 Manual calibration

A manual calibration and sensitivity analysis of the selected updating parameters is very useful for interpretation of the results. Table 2 gives different combinations of foundation stiffness parameters and fig. 8 shows the static results obtained for each combination together with the experimental results.

Case 1 is a simulation of the ideal boundary conditions that would be usually considered during the structural design process (simply supported deck and fixed piers). This "theoretical" approach gives results that are far from the experimental values. The provided displacement values as well as the overall deflection shape are different from the experimental results. If the roof is removed from the FE model (case 1 bis) the contribution of the superstructure of the roof is clear. It is worth to remark that if the superstructure was not considered in the structural design process, the predicted results would be definitely wrong. However, the static deflection of case 1bis is also qualitatively different from the experimental one. So the reason for the difference between the numerical values in case 1 and the experimental ones is not only the contribution of the roof.

If some springs (k_{N-V}, k_{N-L}, $k_{N-\theta VB}$ in fig. 7) are introduced to model more realistically the contribution of the neoprene bearings (case 2), the results are almost identical to the ideal boundary conditions (case 1). Therefore, some additional relaxation of the boundary conditions

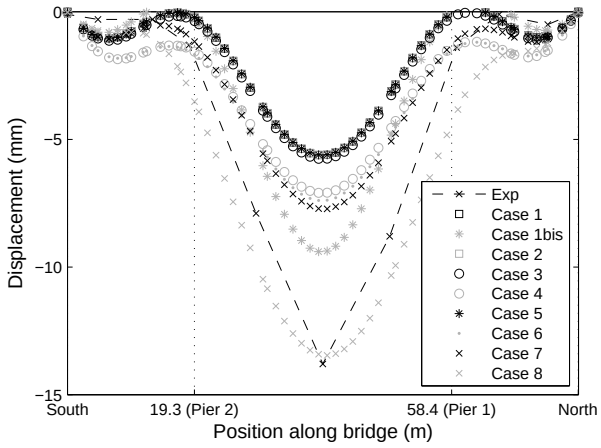

Figure 8: Static displacements for different sets of values of updating parameters according to table 2

is required. As a matter of fact, significant vertical displacements were measured on top of the piers. If the bridge response is analyzed assuming that the structural elements have infinite axial stiffness (which is reasonably close to reality), the only explanation for these vertical displacements is a displacement of the foundation of the piers. Since this foundation is composed of vertical piles and the piers are inclined, horizontal reactions are transmitted to the foundation and the most likely foundation displacement is a horizontal one.

Cases 3 and 4 consider the vertical stiffness of the pier foundations (k_{P-V} in fig. 7) and show that real stiffness values should be in the range $[1e9 - 1e8]$N/m, since the experimental static displacements at the piers are much higher than the computed values of case 3 and much lower than those of case 4. Results with $1e9$N/m could be considered equivalent to an infinite stiffness (ideal boundary condition). In the considered range, the computed static displacements are not in agreement with the experimental ones, the deflection shape still being different from the experimental one. Similar conclusions can be drawn from cases 5 and 6 and the effect of rotational springs in the pier foundations.

Finally, cases 7 and 8 show that the displacement values and the deflection shape are very sensitive to the longitudinal stiffness of the pier foundations(k_{P-L} in fig. 7). The equivalent stiffness is likely to be in the range $[1e8 - 1.5e7]$ N/m.

5.2 Optimization of the static model

By giving null values to the weights of residuals in frequencies and mode shapes in eq. (1), the objective function in the optimization process only includes the residuals in static displacements. Table 3 shows the initial values of the updating parameters and the final values that give the optimum value in the updating process.

Fig. 9 shows that the updated model provides a good approximation to the experimental displacements. The most sensitive and relevant parameter is the longitudinal stiffness of the foundation of the piers (k_{P-L}), as predicted from the manual calibration and sensitivity analysis. The rest of the updated parameters are in agreement with their corresponding theoretical values and can assume a rather broad range of values without affecting the optimum solution. Some of them are not sensitive above a certain threshold value, which is equivalent to an infinite value (table 3), since similar results are obtained as in the case of a fixed boundary condition.

Parameter (N,m)	Initial Values	Final Values	Comment
k_{N-V}	5e8	"∞"	$> 5e8$, not sensitive
k_{N-L}	1.5e6	1e7	Medium influence [0.5e7-1.5e7]
$k_{N-\theta VB}$	1e7	1e6	Not sensitive
k_{P-V}	1e8	"∞"	$> 1e9$, not sensitive
k_{P-L}	1.5e7	**2.398e7**	Extremely sensitive
$k_{P-\theta VB}$	1e8	"∞"	$> 1e9$, not sensitive

Table 3: Results for updating parameters of static response

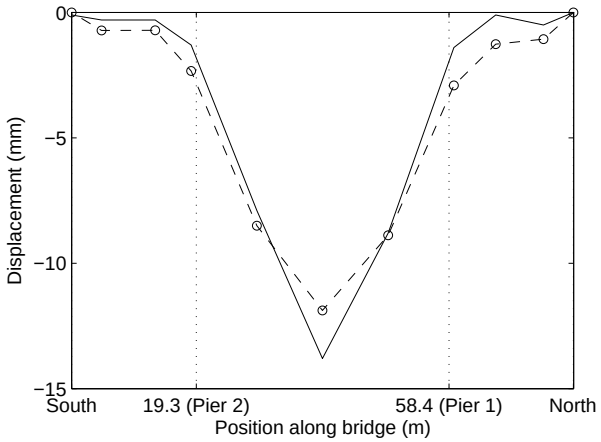

Figure 9: Static displacements of the updated model (o) according to the static experimental displacements (solid line)

Mode Exp.	Mode FEM	Description	MAC	Δf (%)
1	1	Tors. + lat. bend.	0.971	-39.0
2	2	Vert. bend.	0.905	-12.8
3	3	Lat. bend.	0.901	-8.1
4	4	Vert. bend.	0.886	-9.13
5	5	Lat. bend + tors.	0.499	-23.8
6	5	Lat. bend + tors.	0.492	-27.3
7	8	Vert. bend.	0.422	-1.14
8	13	Lat. bend.	0.729	20.0
9	9	Vert. bend.	0.614	-7.6
10	23	Tors. + lat. bend	0.665	71.8
11	6	Vert. bend.	0.395	-30.7

Table 4: Dynamic results with updating parameters from the updating of the static response (table 3)

6 UPDATING DYNAMIC AND STATIC RESPONSE

Whereas the previously considered static response affects only the in-plane behavior, the vertical bending modes as well as the rest of the previously presented modes are considered for model updating. These out of plane modes should be included in order to check that realistic results for the overall response of the bridge are obtained. However, the analysis will be focused on the in plane bending modes. The lateral out of plane stiffness of the foundation is now additionally included in the model updating. Transversal springs in the out-of-plane direction with stiffness k_{N-T} and k_{P-T} are introduced for the neoprene bearings of the abutments and the pier foundations respectively.

6.1 Manual calibration of dynamic model

Once the static model has been updated, the natural frequencies and mode shapes can be obtained with the updated parameters presented in the previous section. For doing so, it is considered that the transversal stiffness of the neoprene bearings (k_{N-T}) is similar to the one in the longitudinal direction (k_{N-L}). Table 4 summarizes the corresponding dynamic results and fig. 10(a) shows the MAC matrix between the numerical and experimental mode shapes. The difference in frequencies of table 4 is defined in the same way as the corresponding residual of the objective function (eq. 3) but applying percentages. The model updated according to the static results does no not give a good approximation of the modal parameters.. Low MAC values and large differences in frequencies between computed and experimental values are obtained.

After the manual sensitivity analysis of the updating parameters, it was found that good results are obtained if the piers are considered to be fixed. Table 5 summarizes the results in that case. Computed mode shapes and frequencies are now much closer to the experimental values. Fig. 10(b) shows a better MAC matrix than in the previous case. The increase in MAC values is particularly significant for the in plane behavior of the experimental bending modes 7, 9 and 11.

Mode Exp.	Mode FEM	Description	MAC	Δf (%) (%)
1	1	Tors. + lat. bend.	0.997	-0.46
2	3	Vert. bend.	0.849	12.4
3	2	Lat. bend.	0.984	-28.65
4	4	Vert. bend.	0.876	1.54
5	5	Lat. bend + tors.	0.575	1.96
6	6	Lat. bend + tors.	0.452	-2.77
7	7	Vert. bend.	0.858	6.10
8	12	Lat. bend.	0.741	32.0
9	8	Vert. bend.	0.969	2.54
10	22	Tors. + lat. bend	0.676	79.58
11	15	Vert. bend.	0.936	-26.87

Table 5: Dynamic results with values of parameters from static updating (table 3) at abutments and considering the piers as fixed elements

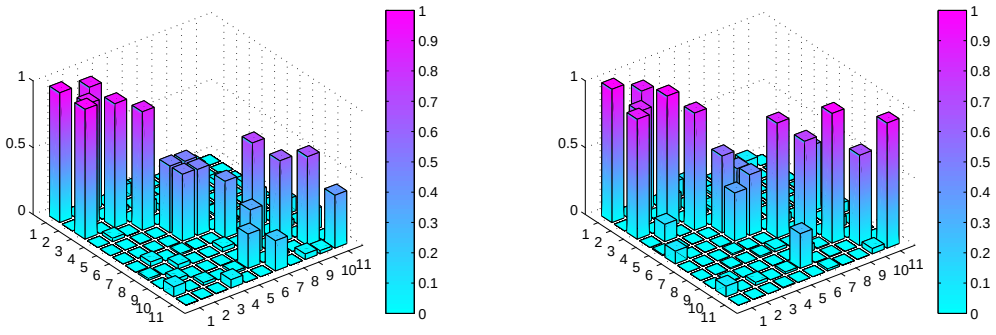

(a) (b)

Figure 10: MAC matrix between experimental modes and computed modes obtained with (a) values of parameters from static updating and (b) the same values but with the piers considered to be fixed

Parameter (N,m)	Initial Values	Final Values	Comment
k_{N-V}	5e9	"∞"	$> 5e8$, not sensitive
k_{N-L}	1.5e7	1.58e7	Sensitive
k_{N-T}	7.5e7	1.51e7	Sensitive
$k_{\theta-VB}$	1e7	2e6	Not sensitive

Table 6: Values of updating parameters at abutments considering the measured static and dynamic response

Mode Exp.	Mode FEM	Description	MAC	Δf (%)
1	1	Tors. + lat. bend.	0.997	-0.50
2	3	Vert. bend.	0.880	13.6
3	2	Lat. bend.	0.983	2.98
4	4	Vert. bend.	0.902	2.19
7	7	Vert. bend.	0.858	-0.08
8	8	Lat. bend.	0.899	-0.43
9	9	Vert. bend.	0.970	-4.79
11	16	Vert. bend.	0.936	8.85

Table 7: Dynamic results with updating parameters at abutments based on the measured dynamic and static response (table 6)

6.2 Optimization of the static and dynamic model

When considering the static and dynamic response, all terms in the objective function in equation (1) are considered. The applied weights were $w_M = 0.5$ for the mode shapes (MAC values), $w_f = 0.2$ for the frequencies and $w_s = 0.2$ for the static displacements. These values provided good convergence and avoided that any term of the objective function dominated the optimization process.

Since the targeted modes are the in plane vertical bending modes, only the most significant lateral and torsional modes are retained in the analysis. Vertical bending modes $(2, 4, 7, 9, 11)$ and lateral and torsion modes $(1, 3, 8)$ were eventually considered.

The updating parameters include only the stiffness of the neoprene bearings at the abutments (k_N). Table 6 includes the corresponding values after updating the FE model. The optimization process gives precise values for the longitudinal (k_{N-L}) and transversal (k_{N-T}) springs, whereas it is not very sensitive to the other two.

Table 7 shows the MAC values and relative frequency differences between the experimental and computed modes in the updated model. The updated finite element model gives high MAC values and low discrepancies in frequencies for the vertical bending modes as well as for the considered lateral and torsional modes. Fig. 11 compares the experimental vertical bending modes and the computed form the updated model.

Despite the fact that good results are obtained for the dynamic behavior, the displacements for the static load case obtained with the updated parameters do not agree well with the experimental results (fig. 12). This figure shows also the results obtained when springs at the bottom

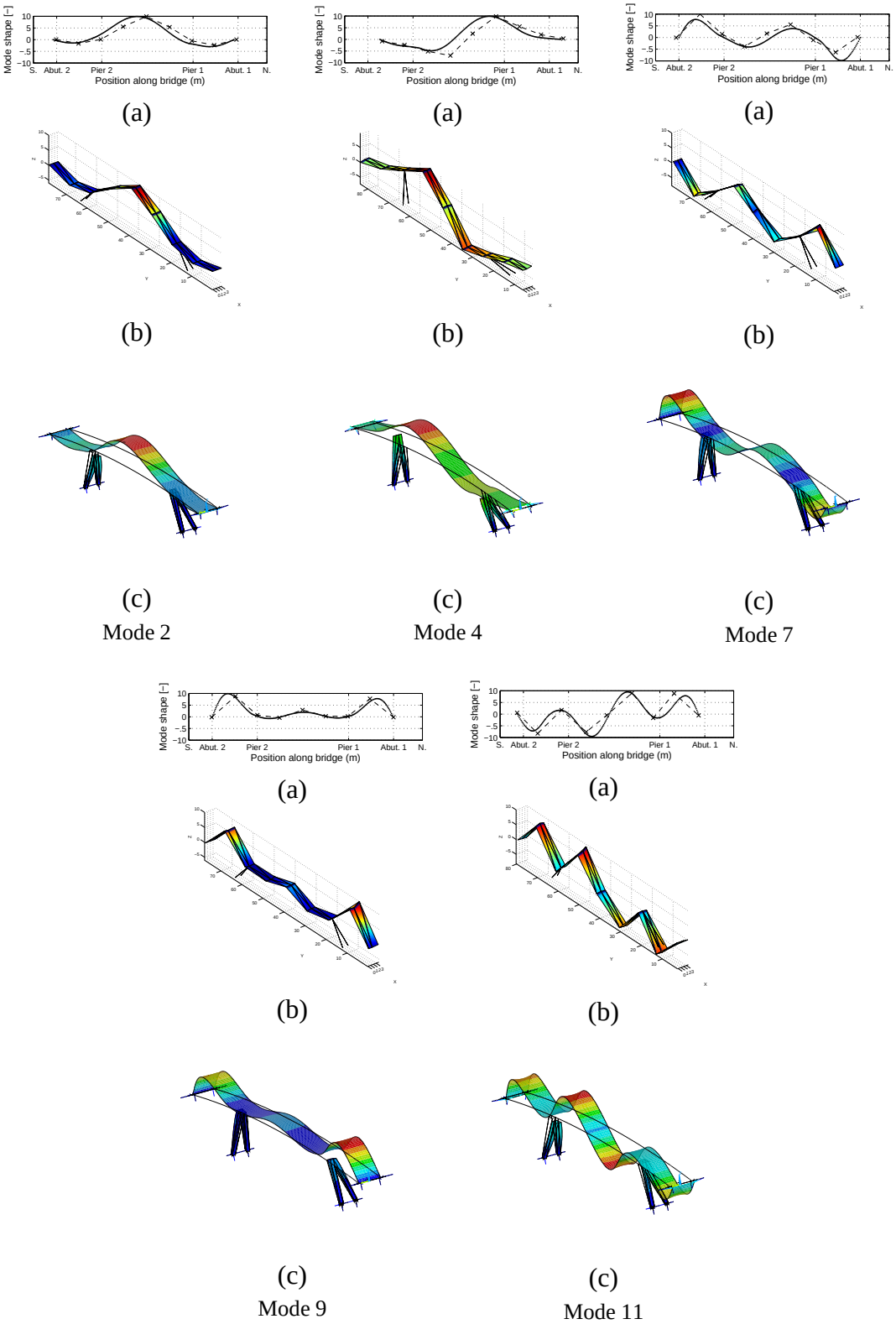

Figure 11: (a)Vertical bending modes from the FE model (solid lines) and experimental ones (discontinuous lines with “x” marks). (b) 3D view of experimental mode shape. (c) 3D view of numerical mode shape (including only deck and piles from the FE model)

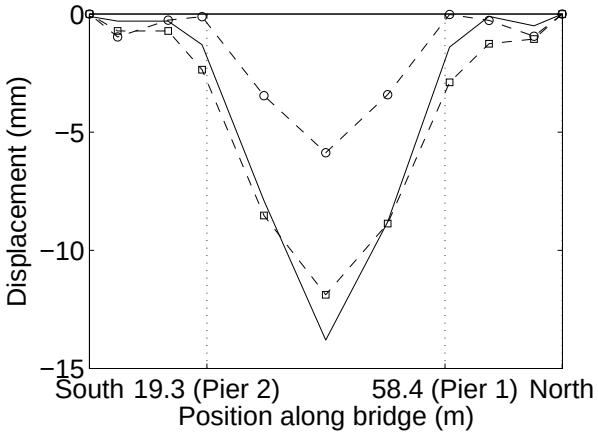

Figure 12: Static displacements from the updated model with fixed piers considering dynamic and static response (o), from the updated model including springs at piers foundation (□) and experimental values (solid line).

of the piers are additionally considered as updating parameters (table 3, fig. 9).

7 DISCUSSION OF RESULTS

The finite element updating process has allowed obtaining a good approximation of either the measured static and dynamic behavior of the bridge. However, compatible bearing stiffness at the abutments have been determined for the static and the dynamic response, whereas non compatibility in the longitudinal stiffness of piers foundation is encountered.

As discussed for the manual calibration of the static model, the measured vertical displacements on top of the piles must be produced by a horizontal displacement of the foundation of the piers. The structural design of the foundation (long vertical piles) and the piers (inclined piers) justifies the low horizontal stiffness at the foundation. Thus, the static model response "needs" a flexible foundation to approach the experimental results.

On the other hand, the dynamic model requires a rigid foundation (infinite stiffness) to simulate the mode shapes and frequencies obtained from the Operational Modal Analysis. The proposed explanation for this is that the mass of the foundation and surrounding soil is sufficiently large to make the foundation behave as a fixed point from a dynamic point of view. In order to address this phenomenon, the FE model should consider an equivalent mass of the foundation and the soil, so mass elements would be introduced as new updating parameters. Thus, static as well as dynamic soil-foundation-structure interaction could be considered and a more accurate updating process could be performed. Ongoing work is focused on the analysis of a new model that accounts for the dynamic soil structure interaction effect.

8 CONCLUSIONS

This paper has successfully combined the static and dynamic experimental response of a footbridge to obtain a finite element model that accurately reproduces the static and dynamic response. The updating process has provided useful information about the actual behavior of the bridge and the interaction with its foundation. The static load test has provided relevant information. The role of the foundation of the piers would probably not have been clear from a dynamic test. In addition, static results are easier and faster to analyze than the dynamic results.

Possible soil-structure interaction effects require further analysis. The finite element model should include a more complex model for the soil and foundation.

9 ACKNOWLEDGEMENTS

This research was funded by the Spanish Ministry of Economy and Competitiveness (*Ministerio de Economía y Competitividad*) through research project BIA2010-14843. Financial support is gratefully acknowledged.

References

[1] P. Dallard, A. J. Fitzpatrick, A. Flint, S. L. Bourva, A. Low, R. M. R. Smith, and M. Willford, "The london millennium footbridge," *Structural Engineer*, vol. 79, no. 22, pp. 17–33, 2001.

[2] S. Zivanovic, A. Pavic, and P. Reynolds, "Vibration serviceability of footbridges under human-induced excitation: a literature review," *Journal of Sound and Vibration*, vol. 279, pp. 1–74, 1/6 2005.

[3] K. L. Structural Mechanics Division, "Macec," *http://bwk.kuleuven.be/bwm/macec*.

[4] B. Peeters and G. D. Roeck, "Reference-based stochastic subspace identification for output-only modal analysis," *Mechanical Systems and Signal Processing*, vol. 13, no. 6, pp. 855–878, 1999.

[5] E. Reynders, J. Houbrechts, and G. D. Roeck, "Fully automated (operational) modal analysis," *Mechanical Systems and Signal Processing*, vol. 29, pp. 228–250, 5 2012.

[6] E. Matta, R. Ceravolo, A. D. Stefano, A. Quattrone, and L. Z. Fragonara, "Structural system identification in the presence of resonant non-structural appendages," in *Proceedings of the Eleventh International Conference on Computational Structures Technology*, 2012.

[7] A. Teughels, *Inverse modelling of civil engineering structures based on operational modal data*. Ph.D. Thesis, Katholieke Universiteit Leuven, 2003.

[8] N. Yazdani, S. Eddy, and C. Cai, "Effect of bearing pads on precast prestressed concrete bridges," *Journal of Bridge Engineering*, vol. 5, no. 3, pp. 224–232, 2000. http://ascelibrary.org/doi/pdf/10.1061/224

[9] AASHTO, *AASHTO LRFD bridge design specifications*. Washington,DC: AASHTO, 1996.